Laboratori Nazionali di Frascati

LNF-67/58

C. Bacci, G. Penso, G. Salvini, C. Mencuccini, A. Reale, V. Silvestrini, M. Spinetti and B. Stella: PHOTOPRODUCTION OF NEUTRAL PIONS FOR INCIDENT PHOTON ENERGIES 400-800 MeV. SEARCH FOR A RESONANT P_{11} STATE AND REMARKS ON THE η CUSP EFFECT.

Estratto da : Phys. Rev. 159, 1124 (1967)

Reprinted from THE PHYSICAL REVIEW, Vol. 159, No. 5, 1124–1137, 25 July 1967
Printed in U. S. A.

Photoproduction of Neutral Pions for Incident Photon Energies 400–800 MeV. Search for a Resonant P_{11} State and Remarks on the η Cusp Effect

C. BACCI, G. PENSO, AND G. SALVINI
Istituto di Fisica dell'Università, Roma, Italy and Istituto Nazionale di Fisica Nucleare, Sezione di Roma, Roma, Italy

AND

C. MENCUCCINI, A. REALE, V. SILVESTRINI, M. SPINETTI, AND B. STELLA
Laboratori Nazionali del Comitato Nazionale per l'Energia Nucleare, Frascati, Italy

(Received 19 December 1966)

Cross sections for the photoproduction of neutral pions have been measured at the 1.1-GeV Frascati electron synchrotron for bombarding photon energies k between 400 and 800 MeV and for π^0 c.m. angles of $\theta_\pi^*=90°$, 120°, and 135°. The main feature of the experiment is good resolution in incident photon energy. The results are in good agreement with the existing theories in the energy range of 450 to 550 MeV. The cross sections exhibit a smooth behavior as a function of energy for $k=400$–600 MeV. No immediate evidence is found of a contribution of the P_{11} resonance. An anomaly at the limit of statistical significance appears for $k\simeq 700$–740 MeV, indicating a possible structure of the so-called second resonance. We attempt to interpret the observed anomaly as a reflection of the sharp opening of the η production channel (η cusp effect).

1. INTRODUCTION

THE first attempts to give a phenomenological interpretation of the pion nucleon (π-N) interaction for a total c.m. energy E^* of the system smaller than $\sim$1800 MeV were done mainly in terms of three resonant amplitudes: the three isobaric states P_{33} (1236 MeV), D_{13} (1518 MeV), and F_{15} (1688 MeV).

However, as new experimental material became more precise and the analysis more detailed, it turned out that this approach is certainly too naive.

The new experimental information came mainly from π-N scattering, which indicated (see Sec. 5 and references quoted therein) that

(a) a P_{11} state, probably resonant, is present and important in the region between the first and the second resonance. Its contribution appears as a broad bump in the cross section for pion-nucleon scattering and is clearly put in evidence in several detailed phase shift analyses;

(b) states other than the ones mentioned are important at energies close to the second resonance: The relative importance of these states is, however, not yet known, large discrepancies being still present among the analyses of different authors.

The understanding of the π-N interaction in this energy region now awaits new experimental data, from pion and photon beams.

In particular, the photoproduction data are rather scanty in the energy region between the first and the second resonance, and the measurements available

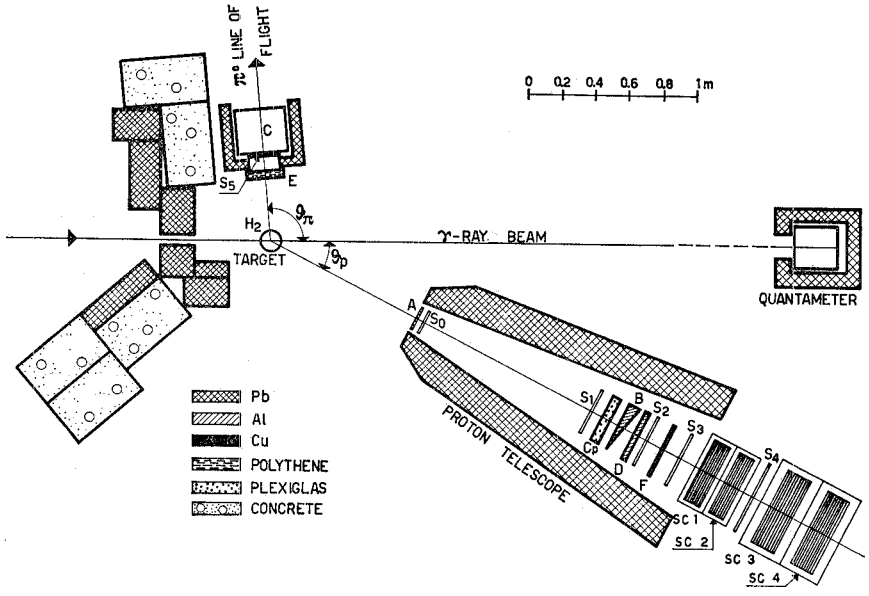

FIG. 1. Experimental layout.

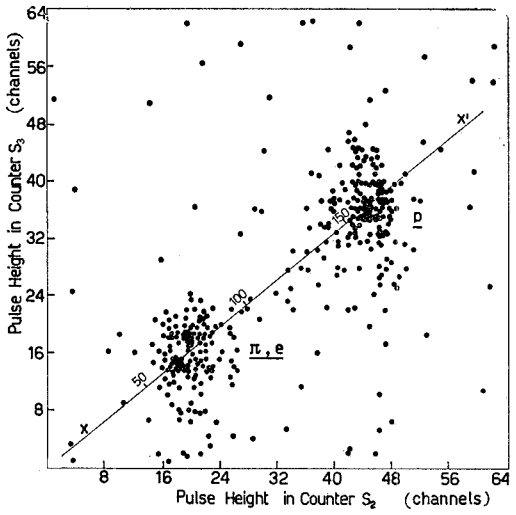

FIG. 2. Bidimensional plot of pulse heights in counters S_2 and S_3. The number of pions and electrons has been increased for demonstration purpose by not requiring a γ ray in coincidence with the proton.

around the second resonance have been performed, apart from few exceptions, with a rather poor energy resolution (see Sec. 5).

In this paper we describe an experimental study of the reaction

$$\gamma+p\rightarrow\pi^0+p \qquad (1)$$

performed at the 1.1-GeV Frascati electron synchrotron, with high energy resolution.

This paper is divided into six sections: In Sec. 2 we describe the experimental layout, in Sec. 3 the criteria used for data reduction. The experimental results are presented in Sec. 4 and discussed in Sec. 5. In Sec. 6 we give our conclusions. In Appendix A we discuss some possible systematic errors; Appendix B, in connection with the discussion of Sec. 5, is devoted to some details on the calculation of a possible η cusp effect.

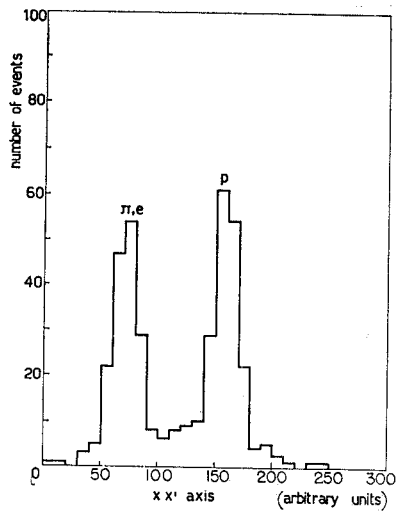

FIG. 3. Distribution of Fig. 2, projected on the xx' axis. Protons are clearly separated from the relativistic particles.

2. EXPERIMENTAL ARRANGEMENT

The experimental lay-out is shown in Fig. 1. It is the same used in an η-photoproduction experiment which has been described with some detail elsewhere.[1] Some details on its use in detecting the photoproduction of π^0's have been presented in Ref. 2.

The γ-ray beam from the Frascati 1.1-GeV electron synchrotron is incident upon a 7.4 cm liquid-hydrogen target.[3]

The proton telescope (PT) (Fig. 1) consists of the scintillators S_0 to S_4, the Plexiglas Čerenkov counter Cp, and the four spark chambers SC1 to SC4. In the spark chambers, the angle and the range of the proton from reaction (1) are measured.

The γ telescope consists of a total-absorption lead-glass Čerenkov counter C, with an anticoincidence scintillator S_5 in front, to eliminate charged particles. The Čerenkov counter C detects γ rays from the π^0's decay, and measures their energy through the pulse

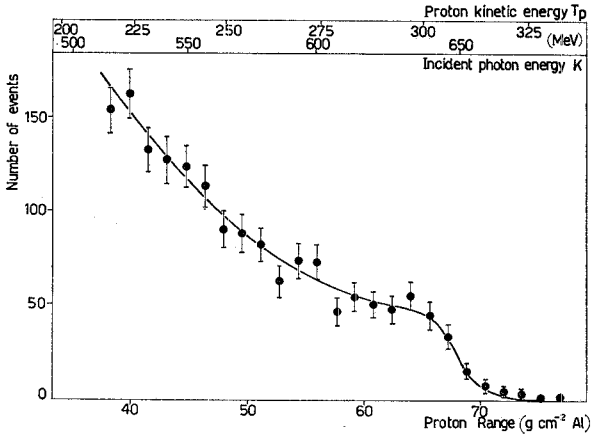

FIG. 4. A proton spectrum as a function of the range. The kinetic energy of the proton and the energy of the photon producing reaction (1) are also indicated (upper scales). The energy E_0 of the synchrotron was 650 MeV and corresponds to the step in the proton-range spectrum.

height produced by gamma-ray showers in the counter. The polythene slab E shields S_5 against low-energy background.

The spark chambers are triggered by a coincidence between a proton in the proton telescope and a photon in the γ-ray telescope. Discrimination against pions and electrons in the proton telescope is obtained by use of the Plexiglas Čerenkov counter Cp in anticoincidence, and of a pulse-height discrimination on S_1.[2] These criteria (in addition to the requirement of a coincidence with a

[1] C. Bacci, G. Penso, G. Salvini, C. Mencuccini, and V. Silvestrini, Phys. Rev. Letters **16**, 157 (1966); **16**, 384 (1966); C. Bacci, C. Mencuccini, G. Penso, G. Salvini, and V. Silvestrini, Nuovo Cimento **45**, 983 (1966).

[2] C. Bacci, C. Mencuccini, G. Penso, V. Silvestrini, M. Spinetti, and B. Stella, Rend. Accad. Naz. Lincei **39**, 452 (1965).

[3] V. Montelatici, Nucl. Instr. Methods **29**, 121 (1964).

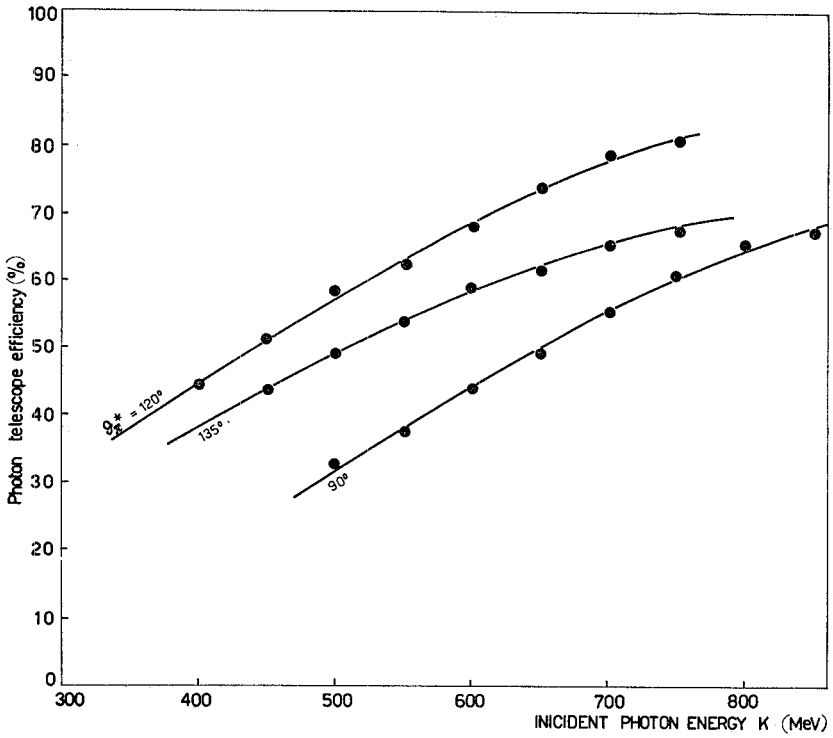

FIG. 5. Čerenkov counter geometrical efficiency of π^0 detection, as obtained by a Monte Carlo calculation. The three curves refer to the three kinematical situations chosen for this experiment. The distance from the H_2 target to the Čerenkov counter C was not the same at the three angles.

photon in C), reduce to 5–10% the contamination of relativistic particles in the triggers to the spark chambers. In addition, the pulse heights in counters S_2 and S_3 are digitized and recorded on each photograph. This information allows complete elimination of pions and electrons when analyzing the data, as we describe in detail in the next section.

The pulse height of Čerenkov counter C is also digitized and recorded on each photograph.

The Čerenkov counter C has been calibrated by using monochromatic electrons from a pair spectrometer.

The beam intensity is monitored by a Wilson quantameter.[4] Since the counting rate in this experiment is rather high (~1 event per sec = 1 event per 20 machine pulses) and the advance of the film takes $\sim\frac{1}{3}$ sec, a substantial correction to the beam flux should be applied to correct for dead time. In order to reduce this

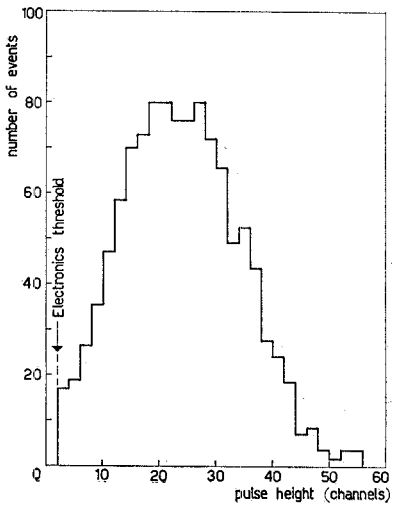

FIG. 6. Pulse-height distribution in C of the photons in coincidence with the protons in a small range interval. The number of events which are lost due to the electronics threshold of C is typically 5÷10%.

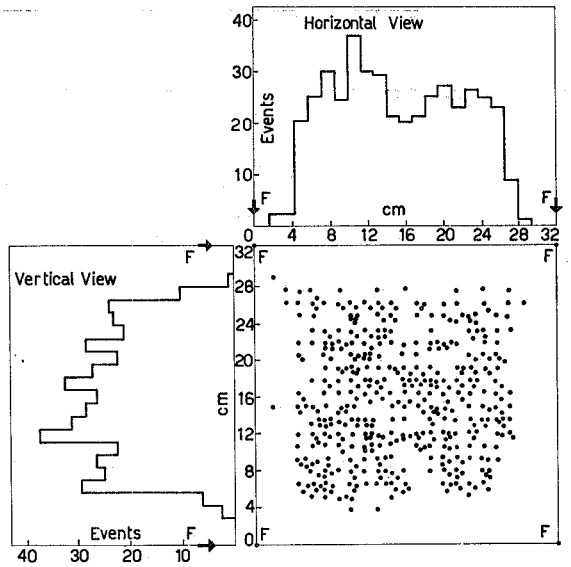

FIG. 7. Distribution of the protons entering SC1 as a function of the entrance coordinates. This distribution fits well the shadow from the H_2 target of counter $S3$, defining the solid angle. The fiducial marks F indicate the useful area of the spark chambers.

[4] R. R. Wilson, Nucl. Instr. Methods **1**, 101 (1957).

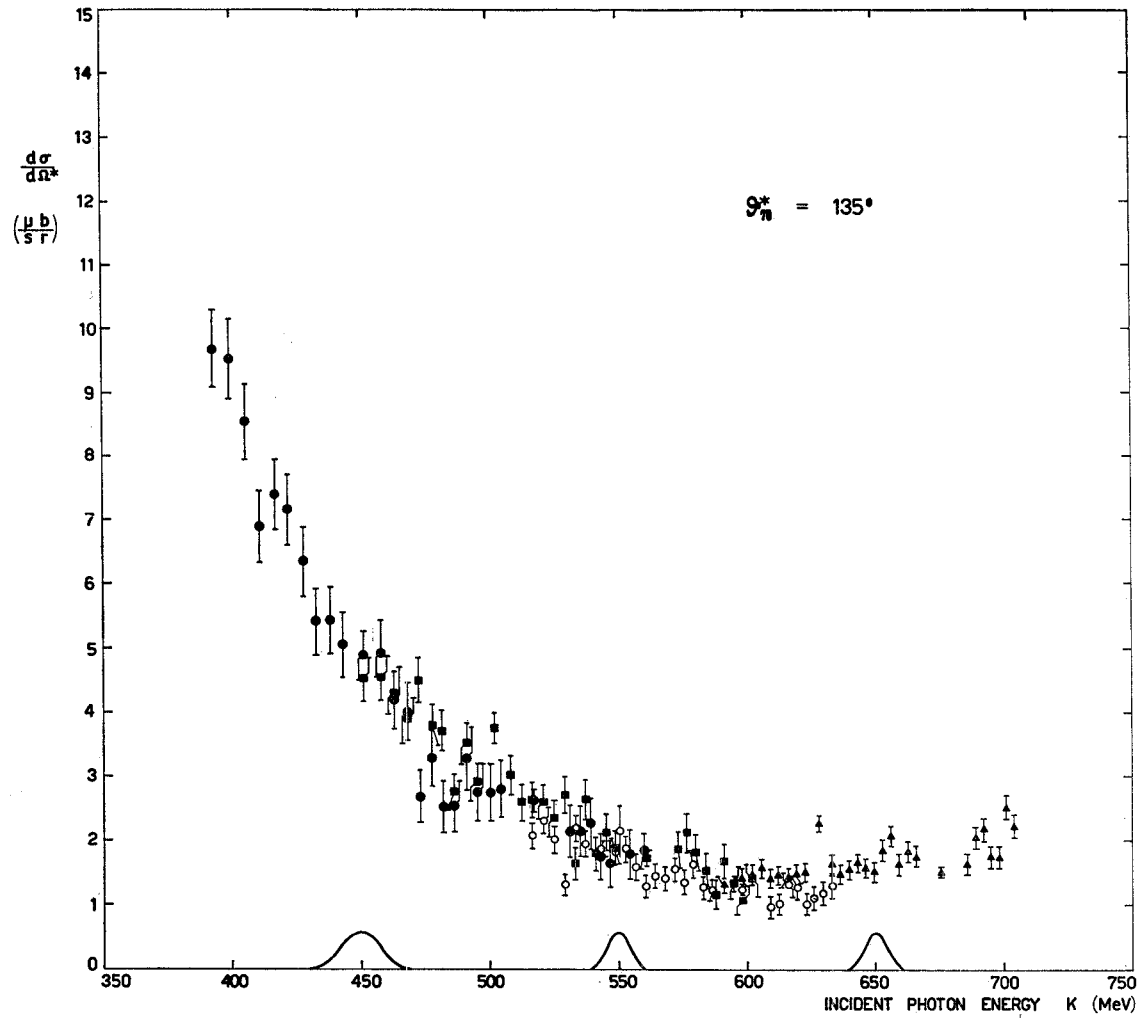

FIG. 8. Present experimental results at $\theta_\pi^* = 135°$. Results obtained with different values of the machine energy E_0 are presented separately. The energy resolution is also shown. ● $E_0 = 580$ MeV; ■ $E_0 = 620$ MeV; ○ $E_0 = 650$ MeV; ▲ $E_0 = 730$ MeV.

effect, the synchrotron injection is gated off while the film is advancing. In this way the dead-time effect is reduced to ~5%, corresponding to events which are produced during the same machine pulse. We corrected our data for this effect.

The wedge-shaped aluminum absorber B in the proton telescope (Fig. 1) compensates approximately for the dependence of the energy of the recoil protons on their emission angle. A correspondence between the range of the proton and the incident photon energy is thus obtained sufficiently well at 120° and 135° (see Fig. 14). For the analysis of the 90° data both the angle and energy of the proton were used.

3. DATA REDUCTION

The first problem to be solved when analyzing the data is to eliminate pions and electrons from the particles detected in the proton telescope. As we said, the electronics requirements on the triggers of the spark chambers already reduce to 5-10% the contamination of relativistic particles.

The information at our disposal which allows us to eliminate pions and electrons completely is the range of the particle in the spark chambers and the pulse heights in counters S_2 and S_3.

For each set of particles whose range differs by less than ~2 g/cm², we plot a two-dimensional distribution of the pulse heights from counters S_2 and S_3. A typical bidimensional pulse-height plot is shown in Fig. 2. The number of pions and electrons in this sample has been increased for demonstration purposes by not requiring a coincidence with a γ ray in C. By projecting this plot on the xx' axis of Fig. 2 the pulse-height distribution of Fig. 3 is obtained. The elimination of relativistic particles can be performed in this way with ~1% accuracy with respect to the number of detected protons.

Once pions and electrons have been eliminated, the accepted events are plotted in a two-dimensional

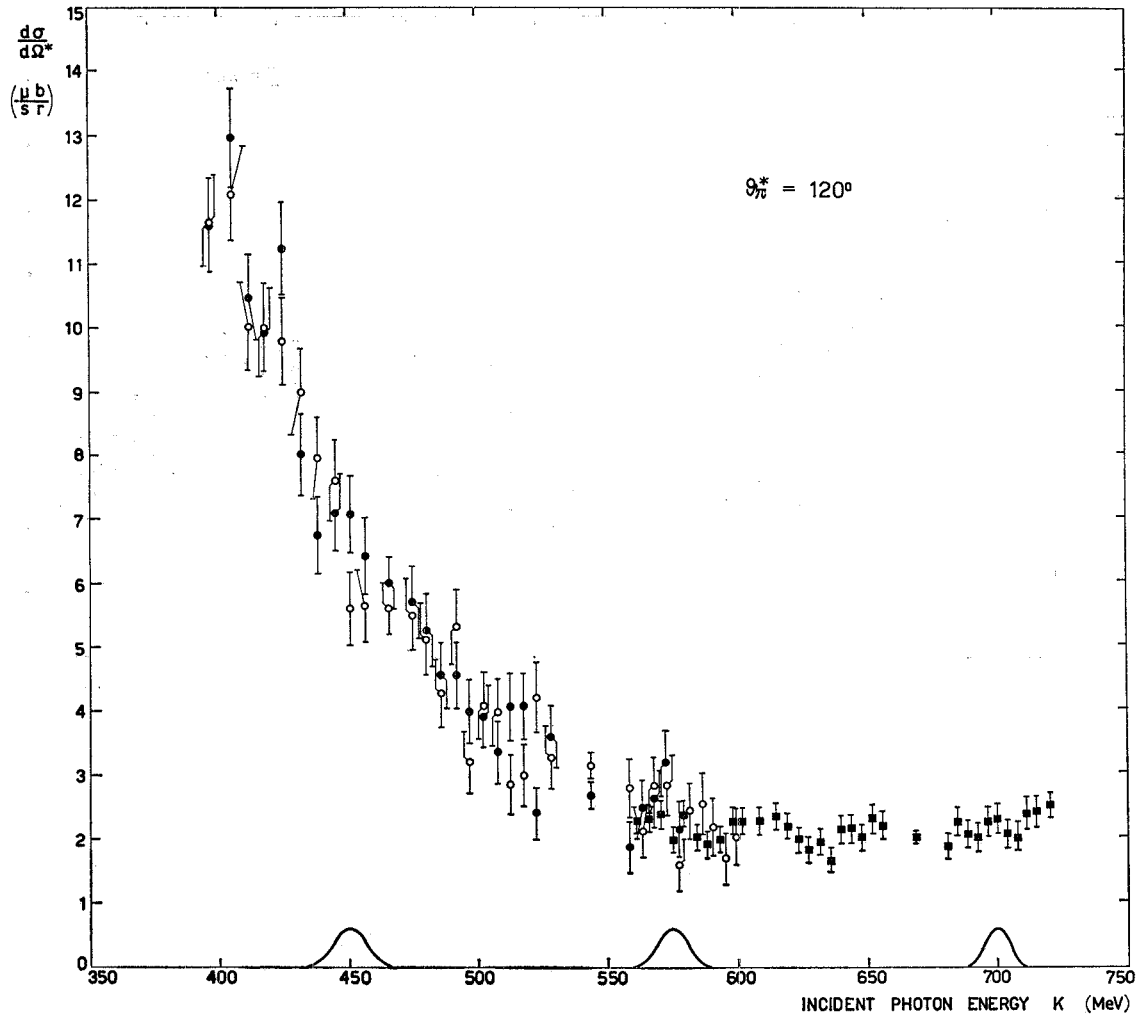

FIG. 9. Present experimental results at $\theta_\pi^* = 120°$. Results obtained with different values of the machine energy E_0 are presented separately. The energy resolution is also shown. ● $E_0 = 590$ MeV; ○ $E_0 = 620$ MeV; ■ $E_0 = 740$ MeV.

distribution in the variables proton range and photon energy observed in C.

A typical projection of such a plot on the proton-range axis is reported in Fig. 4.

The spectrum obtained by projection on the proton-range axis is strictly related to the cross section for process (1). In fact, apart from corrections discussed in the following, the shape of this distribution is an image of the spectrum of the incident bremsstrahlung beam, weighted by the cross section of reaction (1).

As a consequence, once the angle of the proton telescope is fixed, each set of our measurements (a set being defined by a particular choice of the machine energy and of the absorbers in the PT) provides values of the cross section over a rather large range of k (100–200 MeV). This point is important since most systematic errors in the relative normalization of the data points are avoided in this way. By changing the machine energy E_0 (and possibly the absorbers in the PT) another interval of k is explored, which is generally chosen so as to be partially overlapped with the previous one. The agreement between cross sections from two or more sets (Figs. 8–10) in the overlapping region checks against possible normalization errors in different sets.

Once the proton spectrum has been obtained the following corrections are applied:

(a) *Subtraction of empty target background and accidental rate.* Each of these corrections is of the order of 3–5%;

(b) *Correction due to nuclear interactions of the protons in the telescope and in the spark chambers.* We use a mean free path of 110 g/cm^2 as extracted from Millburn *et al.*[5] The method used to apply this correction is described in detail in Ref. 2. We take into account, of course, both the fact that the effective number of protons which would stop in a given spark chamber plate is lowered by the nuclear interactions in the preceding absorber, and that it is enhanced by the nuclear

[5] G. P. Millburn, N. Birnbaum, W. E. Crandall, and L. Schecter, Phys. Rev. **95**, 1268 (1954).

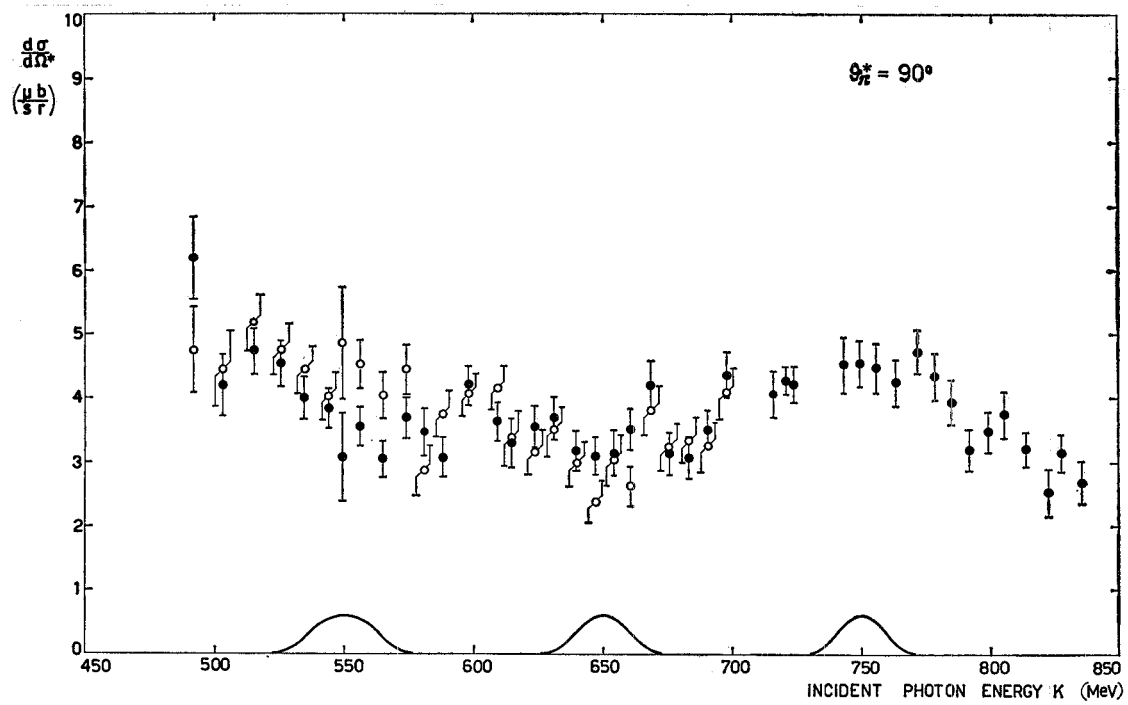

FIG. 10. Present experimental results at $\theta_\pi^*=90°$. The results of the two measurements performed at $E_0=850$ and 750 MeV are presented separately. The energy resolution is also shown. ● $E_0=850$ MeV; ○ $E_0=750$ MeV.

interactions of the proton in the plate considered from the protons which would stop in the following plates. This correction is, in some situations, as high as 30% (in the highest energy points at $\theta_\pi^*=135°$).

(c) *Correction due to the efficiency of detection of the π^0 decay gammas by C.* The geometrical efficiency has been evaluated by means of a Monte Carlo calculation,[2] and it is typically 40–60% (Fig. 5). Another effect we have taken into account is the possibility that a π^0 is not detected by the electronics, which happens if it gives rise to too small a pulse height in C. However, if the electronics threshold on C is set too low, the accidental rate becomes too large. We have set this threshold at a photon energy of ~80 MeV. To determine the correction for π^0's lost because of this threshold, we have plotted the pulse-height distribution in C for photons in coincidence with protons belonging to small range intervals. A typical spectrum of this kind is shown in Fig. 6. Depending on the kinematical situation, this correction goes from $\sim(5\pm3)\%$ to $\sim(10\pm6)\%$ (see Appendix A).

(d) *Losses due to multiple scattering in the telescope.* This effect has been computed and has turned out to be negligible in our geometry. A check of this can be obtained by plotting the events as a function of their entrance point in the spark chambers. A rectangular distribution has been obtained (Fig. 7), which is the shadow from the H_2 target of counter $S3$, which defines the solid angle. This plot also checks for counter misalignments.

(e) *Contamination from multipion production.* Once the proton telescope has been set at an angle θ_p, the energy k of the photon which produces reaction (1) is uniquely related with the energy of the proton detected in the telescope. By properly choosing the absorbers in the proton telescope and the machine energy E_0, it is possible to select k in such a way that

$$(E_0-100\text{ MeV})\leq k\leq E_0. \qquad (2)$$

This energy region is kinematically free from multipion production. Unless the energy distribution of protons from multipion production is strongly peaked towards the high energies, it is to be expected that the region free from multipion production extends to values of k somewhat smaller than indicated by relation (2). Our data with $\theta_\pi^*=120°$ and $\theta_\pi^*=135°$ were collected in many sets of measurements. The values of E_0 and the absorbers in the PT were set in such a way as to satisfy, in each set of measurements, relation (2), except for the points at the lowest energies in each set, which are, however, superimposed with points from another measurement which satisfy relation (2). The comparison between the results of the different set of measurements (Figs. 8 and 9) allows us to conclude that the contamination from multipion production is, if any, very small (of the order of a few percent).

The data with $\theta_\pi^*=90°$ were collected in two sets of measurements with $E_0=850$ and 750 MeV (Fig. 10). Contamination from multipion production could thus be present in the first set for $k<750$ MeV and in the second for $k<650$ MeV, giving, therefore, at low energy, higher cross sections for the set with $E_0=850$

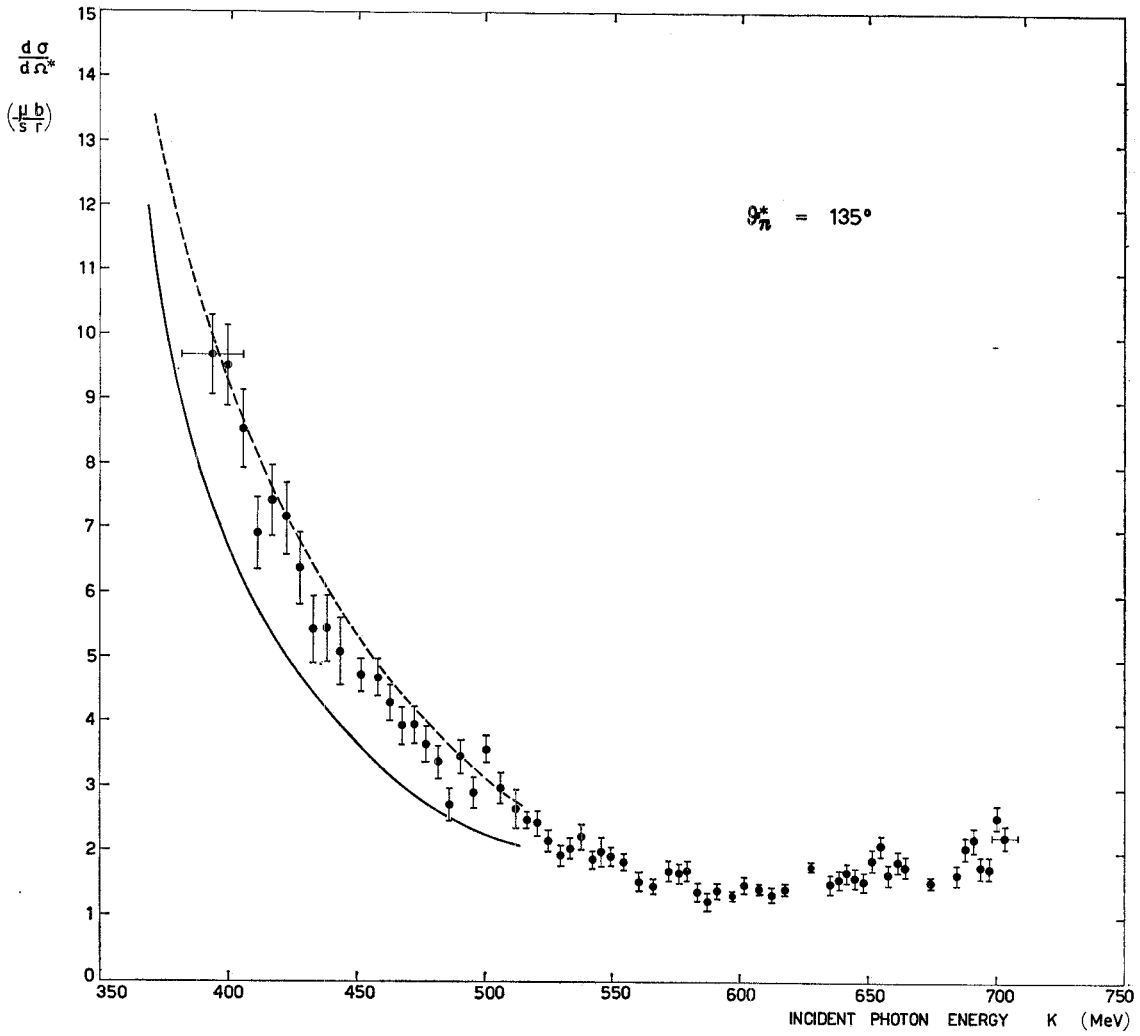

FIG. 11. Differential-cross-section results at $\theta_\pi^* = 135z$. The different sets of measurements of Fig. 8 have been averaged (see Ref. 8). The dashed and full lines are the theoretical calculations by Schmidt (Ref. 12) and Donnachie and Shaw (Ref. 13), respectively. The energy resolution is shown on the first and last point.

MeV. However, since the data collected with $E_0 = 750$ MeV are consistent within statistics with those with $E_0 = 850$ MeV, we considered the contribution from multipion production negligible also in this case.

(f) *Contribution of the Compton effect on protons.* A correction should be applied to our data in order to take into account the contamination from the elastic scattering of photons:

$$\gamma + p \rightarrow \gamma + p. \quad (3)$$

This process is not distinguishable from reaction (1), since the kinematics of the two reactions are very similar. However, the cross section for process (3) is of the order of 2%[6,7] of the cross section for process (1). Since the efficiency of our Čerenkov counter for detecting the γ ray from process (3) is ~100%, while the efficiency of detection of a γ-ray from process (1) is ~50%, there is in our results a contamination of ~4% from process (3). We have not attempted to separate this contamination.

(g) *Dead-time corrections.* As we said, the main part of this correction is automatically done by stopping the synchrotron while the film is advancing. However, if two good events are produced during the same machine pulse, the second one is lost. A correction for this effect is applied to the data, by comparing the number of photographs with the number of events recorded on a scaler. This correction is of the order of 5%.

(h) Photographs containing two tracks, or which were for some other reason not completely measurable, were disregarded at the scanning table. A correction for this effect (~2%) was applied to the final data.

[6] R. F. Stiening, E. Loh, and M. Deutsch, Phys. Rev. Letters **10**, 536 (1963).
[7] D. R. Rust, E. Eisenhandler, P. J. Mostek, A. Silverman, C. K. Sinclair, and R. M. Talman, Phys. Rev. Letters **15**, 938 (1965).

(i) In connection with our conclusions (compare Sec. 5), some points of the measurement at $\theta_\pi^*=90°$ (the ones between $k=680$ and $k=750$ MeV) are of particular importance. For this reason these data were handled with particular care. The scanning was performed three times independently by different scanners, obtaining consistent results, and a correction was applied for the efficiency of the single gaps.

Once all these corrections have been applied to the experimental data, the corrected plot of the number of events versus proton range is obtained. This plot is transformed into a plot $N(T_p)$ of the number of events versus proton kinetic energy T_p. The cross section for process (1) is then obtained through the relation

$$\frac{d\sigma}{d\Omega^*}=\frac{N(T_p)(dT_p/dk)}{[b(k/E_0)/k]\,(d\Omega^*/d\Omega)\Delta\Omega\, n\, Q},$$

where T_p is the kinetic energy of the proton, k is the energy of the incident photon, $N(T_p)$ is the number of events per unit interval of T_p, Q is the number of equivalent quanta used to collect the data, as measured by the Wilson quantameter, $b(k/E_0)/k$ is the shape of the bremsstrahlung spectrum (the Bethe-Heitler formula has been used, corrected for the thickness of the synchrotron internal target), n is the number of atoms/cm^2 of the H_2 target and $\Delta\Omega$ is the solid angle of our proton telescope (6.7 msr). The derivatives dT_p/dk and $d\Omega^*/d\Omega$ are calculated at fixed θ_p and k respectively.

4. EXPERIMENTAL RESULTS

The experimental results are presented in Figs. 8–13. In Figs. 8–10 the results of sets of measurements performed at different values of the machine energy E_0 are presented separately: The consistency among them is good.

In Figs. 11–13 and Tables I–III our results are reported, after averaging according to the Crawford's procedure[8] the different sets of measurements which were presented separately in Figs. 8–10.

The errors are only statistical. In fact, the systematic errors we could think of have a smooth behaviour as a function of energy; they cannot raise or destroy any possible "fine-structure" effects, but they affect the absolute normalization of our results. These errors will be discussed in Appendix A.

Our discussion of the possible presence of resonance or fine structures will be based on the results and errors presented in Figs. 11–13. In the same figures, our resolution in the energy of the incident photon is also indicated.

The kinematical regions covered by our results are shown in Fig. 14, from which one can see that our c.m. angular resolution is $\pm5°$.

[8] F. S. Crawford, Jr., Nucl. Instr. Methods 33, 332 (1965).

TABLE I. Differential cross sections in the c.m. system for the process $\gamma+p\rightarrow\pi^0+p$. Experimental results at $\theta_\pi^*=135°$ versus the energy k of the incident photon. (See Fig. 11).

k (MeV)	$d\sigma/d\Omega^*$ (μb/sr)	k (MeV)	$d\sigma/d\Omega^*$ (μb/sr)
394	9.68±0.62	561	1.53±0.14
400	9.53±0.62	566	1.45±0.13
406	8.53±0.60	572	1.68±0.16
411	6.90±0.56	576	1.65±0.15
417	7.39±0.57	580	1.69±0.16
422	7.16±0.57	584	1.37±0.14
428	6.37±0.55	587	1.22±0.14
433	5.42±0.52	591	1.39±0.11
438	5.45±0.52	597	1.31±0.06
444	5.07±0.51	602	1.47±0.12
452	4.71±0.25	608	1.41±0.08
458	4.67±0.28	613	1.32±0.10
463	4.28±0.28	618	1.41±0.08
468	3.93±0.27	628	1.76±0.06
472	3.94±0.27	636	1.47±0.13
477	3.64±0.26	640	1.57±0.14
482	3.37±0.26	643	1.66±0.14
487	2.70±0.23	646	1.58±0.14
491	3.45±0.26	649	1.51±0.14
495	2.89±0.24	653	1.86±0.15
501	3.56±0.21	656	2.08±0.16
506	2.96±0.25	659	1.61±0.14
512	2.65±0.29	662	1.82±0.15
517	2.47±0.12	666	1.75±0.15
521	2.43±0.17	676	1.53±0.06
525	2.15±0.16	686	1.64±0.15
530	1.93±0.15	689	2.06±0.16
534	2.03±0.15	692	2.20±0.17
538	2.22±0.16	695	1.77±0.16
542	1.86±0.12	698	1.75±0.16
546	1.98±0.22	701	2.52±0.19
549	1.90±0.15	704	2.22±0.18
555	1.83±0.13		

TABLE II. Differential cross sections in the c.m. system for the process $\gamma+p\rightarrow\pi^0+p$. Experimental results at $\theta_\pi^*=120°$ versus the energy k of the incident photon. (See Fig. 12).

k (MeV)	$d\sigma/d\Omega^*$ (μb/sr)	k (MeV)	$d\sigma/d\Omega^*$ (μb/sr)
397	11.68±0.51	580	2.41±0.18
404	12.57±0.53	585	2.15±0.18
411	10.33±0.49	589	1.96±0.17
418	9.99±0.48	594	1.95±0.17
425	10.57±0.50	598	2.27±0.18
431	8.52±0.46	608	2.32±0.12
438	7.35±0.43	619	2.20±0.21
444	7.37±0.44	623	2.00±0.20
450	6.38±0.42	627	1.84±0.19
456	6.06±0.41	631	1.97±0.20
465	5.82±0.29	636	1.68±0.19
474	5.61±0.40	640	2.16±0.21
480	5.21±0.40	644	2.18±0.21
486	4.43±0.37	648	2.04±0.20
491	4.94±0.39	652	2.33±0.22
496	3.62±0.35	656	2.22±0.21
502	4.01±0.36	668	2.04±0.09
507	3.67±0.35	681	1.90±0.20
512	3.48±0.34	685	2.28±0.22
517	3.54±0.35	688	2.08±0.21
523	3.35±0.34	692	2.03±0.21
528	3.46±0.35	696	2.28±0.23
543	2.84±0.14	700	2.33±0.23
558	2.36±0.25	704	2.09±0.22
562	2.32±0.17	707	2.06±0.22
667	2.45±0.17	711	2.41±0.24
572	2.57±0.18	715	2.44±0.25
576	1.97±0.16	720	2.55±0.18

TABLE III. Differential cross sections in the c.m. system for the process $\gamma+p\rightarrow\pi^0+p$. Experimental results at $\theta_\pi^*=90°$ versus the energy k of the incident photon. (See Fig. 13).

k (MeV)	$d\sigma/d\Omega^*$ (μb/sr)	k (MeV)	$d\sigma/d\Omega^*$ (μb/sr)
491	5.62±0.47	668	4.04±0.26
503	4.31±0.38	676	3.19±0.23
515	4.94±0.28	683	3.19±0.24
525	4.63±0.27	691	3.40±0.24
534	4.20±0.24	698	4.25±0.27
544	3.92±0.23	716	4.06±0.36
549	3.91±0.55	721	4.26±0.22
556	3.98±0.24	724	4.22±0.27
565	3.50±0.23	743	4.53±0.44
574	4.02±0.24	749	4.56±0.36
581	3.19±0.27	756	4.48±0.36
588	3.39±0.23	763	4.25±0.36
598	4.15±0.22	772	4.73±0.35
609	3.88±0.23	778	4.38±0.37
614	3.34±0.28	784	3.96±0.36
624	3.39±0.24	791	3.21±0.33
631	3.61±0.24	799	3.50±0.31
639	3.10±0.23	805	3.77±0.36
647	2.81±0.22	814	3.22±0.27
654	3.10±0.27	822	2.55±0.36
661	3.15±0.23	827	3.17±0.31
		835	2.71±0.33

5. DISCUSSION OF RESULTS

The consistency of our results with those available up to now (with lower resolution) is rather good. For a comparison, we have reported in Figs. 12 and 13 ($\theta_\pi^*=120°$ and 90°), along with our results, the results of the available experiments in which both proton and γ were detected in coincidence.[9,10,11] No coincidence experiment was available at 135°. Experiments performed without the detection of the π^0 give similar results, apart from the fact that they are systematically somewhat higher.

For $600\lesssim k\lesssim 700$ MeV, our data at 120° are somewhat lower than the results of other experiments. We have no definite explanation for this effect. An overestimate of the mean free path for nuclear absorption of protons in the telescope would give an effect in this direction (see Appendix A).

For the following phenomenological discussion of our data, it is convenient to divide the energy interval we explored (400–800 MeV) into two parts. The first refers to energies $400\lesssim k\lesssim 500$ MeV: This part has been treated quite thoroughly with theoretical approaches and multipole analysis.[12,13] Beyond 550 MeV the situation cannot yet be described in terms of a definite set of multipoles and final states, due to the still insufficient experimental information. We shall therefore analyze our results in terms of a comparison with the results of other reaction channels. The experimental facts which we shall take into account are mainly the increasing evidence of a P_{11} π-N resonance and the photoproduction of the η particle.

For $k\lesssim 550$ MeV, the agreement of our results with the available theoretical predictions (full and dashed lines of Figs. 11–13) is considerably good. The models used by Schmidt[12] and Donnachie *et al.*[13] to make their predictions are based on the use of the fixed t dispersion relations. Since, in addition to other approximations, they neglect in the integrals the imaginary part of the M_{1-} multipole (responsible for the P_{11} state) and of the higher multipoles, it is remarkable that their predictions are in such good agreement with the experimental points. Perhaps an upper limit for the amplitude of this "resonating" M_{1-} multipole could be calculated.

Looking now at the energy interval from 550 to 650 MeV, we first observe that our cross sections do not exhibit any evident bump or anomaly while descending from the first resonance towards a significant minimum between 600 and 650 MeV, and rising again towards a maximum which is usually considered as the "second resonance" or D_{13} state. This behavior is similar to

TABLE IV. Differential cross section in the c.m. system for the process $\gamma+p\rightarrow\pi^0+p$ at $\theta_\pi^*=90°$ versus the energy k of the incident photon (Fig. 15); experiments performed with good energy resolution.

k (MeV)	$d\sigma/d\Omega^*$ (μb/sr)	Ref.	k (MeV)	$d\sigma/d\Omega^*$ (μb/sr)	Ref.
653	3.34±0.15	b	784	3.96±0.36	a
654	3.10±0.27	a	789	4.26±0.23	b
661	3.15±0.23	a	791	3.21±0.33	a
665	3.25±0.13	b	799	3.50±0.31	a
668	4.04±0.26	a	800	3.50±0.10	c
676	3.19±0.23	a	804	4.04±0.21	b
678	3.30±0.11	b	805	3.77±0.36	a
680	3.37±0.11	c			
683	3.19±0.24	a			
691	3.40±0.24	a			
692	3.37±0.13	b			
698	4.25±0.27	a			
700	4.09±0.12	c			
703	3.96±0.15	b			
716	4.06±0.36	a			
720	4.48±0.13	c			
720	4.02±0.15	b			
721	4.26±0.22	a			
724	4.22±0.27	a			
736	4.10±0.20	b			
740	4.29±0.13	c			
743	4.53±0.44	a			
749	4.56±0.36	a			
753	4.67±0.20	b			
756	4.48±0.36	a			
760	4.70±0.14	c			
762	4.88±0.20	b			
763	4.25±0.36	a			
772	4.73±0.35	a			
776	4.87±0.21	b			
778	4.38±0.37	a			
780	4.35±0.13	c			

[a] Present results. [b] Reference 27. [c] Reference 28.

[9] R. Diebold, Phys. Rev. **130**, 2089 (1963).

[10] J. M. DeWire, H. E. Jackson, and R. Littauer, Phys. Rev. **110**, 1208 (1958).

[11] To make Fig. 13 clear enough, we were compelled to omit the results of some old experiments. Complete references can be found, for instance, in R. Diebold, Phys. Rev. **130**, 2089 (1963).

[12] W. Schmidt, Z. Physik **182**, 76 (1964).

[13] A. Donnachie and G. Shaw, Ann. Phys. (N. Y.) (to be published).

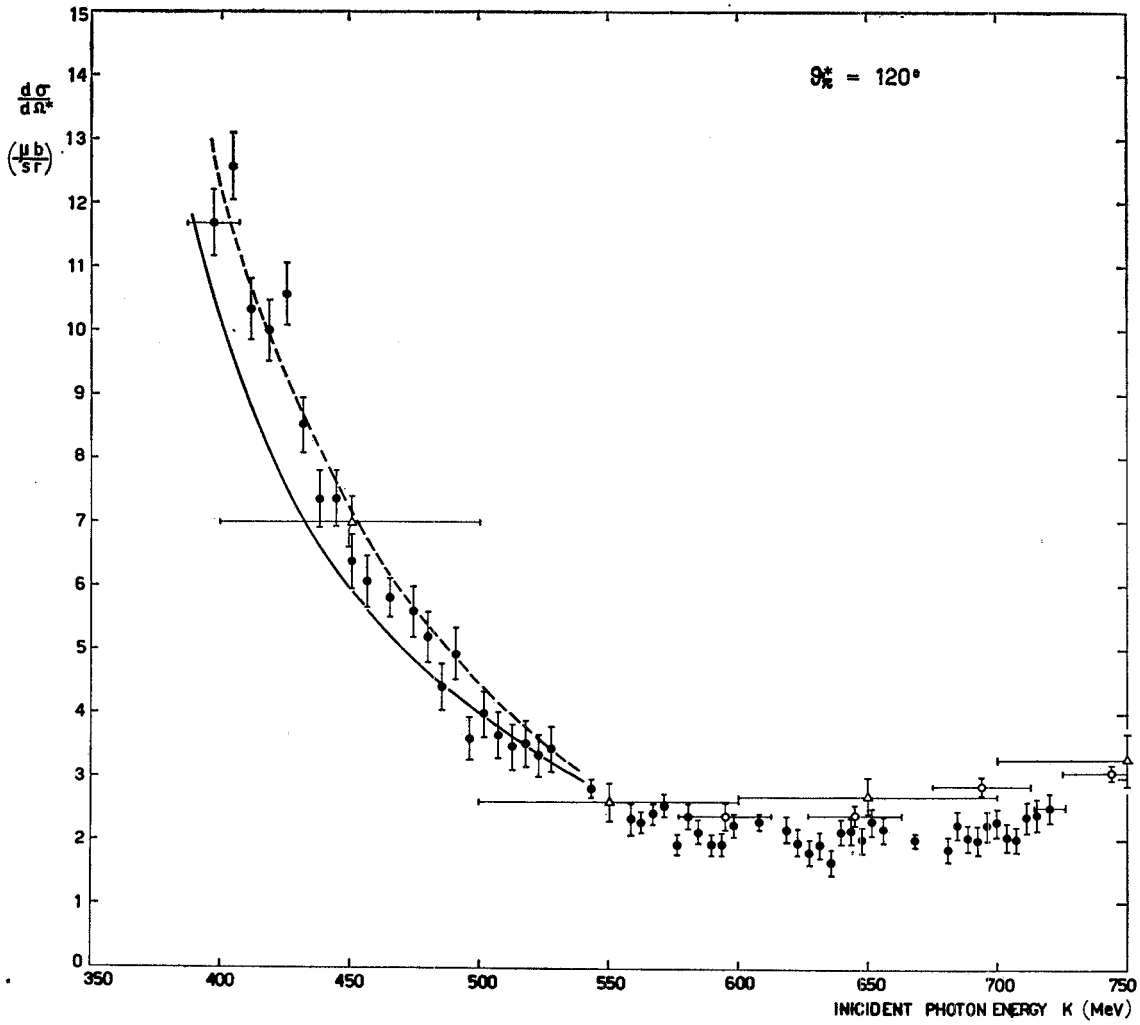

FIG. 12. Differential cross section results at $\theta_\pi^* = 120°$. The different sets of measurements of Fig. 9 have been averaged (see Ref. 8). Results of previous p-π^0 coincidence experiments are also reported. The results of De Wire *et al.* (Ref. 10) refer to $\theta_\pi^* = 125°$. The dashed and full lines are theoretical calculations by Schmidt (Ref. 12) and Donnachie and Shaw (Ref. 13) ● Present results; ○ Ref. 9; △ Ref. 10. The energy resolution of present results is shown on the first and last point.

what is observed at smaller angles.[14] We recall that in this energy region the P_{11} "resonance" is expected to show up. However, the position and nature of this "resonance" is not yet established. It was observed as a bump in the π-N cross section or in a π-N invariant mass spectrum[15–17] at ~1410 MeV. Phase-shift analyses have confirmed the importance of the P_{11} state: Some of these support the hypothesis of a resonance (essentially inelastic), giving however, in general, a higher value for its mass: 1425 MeV[18]; 1485 MeV[19]; and 1510 MeV.[20–23] In other analyses, a phenomenological interpretation of the π-N interaction is given, not requiring the P_{11} state to resonate.[24,25] Also the width of this "resonance" is not established, different authors giving values ranging from 60–250 MeV.

[14] G. Bellettini, C. Bemporad, P. J. Biggs, P. L. Braccini, T. Del Prete, and L. Foà, Nuovo Cimento 44, 239 (1966).
[15] P. Bareyre, C. Bricman, G. Valladas, G. Villet, J. Bizard, and J. Seguinot, Phys. Letters 8, 137 (1964).
[16] G. Cocconi, E. Lillethum, J. P. Scanlon, C. A. Stahlbrandt, C. C. Ting, J. Walters, and A. M. Wetherell, Phys. Letters 8, 134 (1964); G. Bellettini, G. Cocconi, A. N. Diddens, E. Lillethum, J. P. Scanlon, and A. M. Wetherell, in *Proceedings of the International Symposium on Electron and Photon Interactions at High Energies*, edited by G. Höhler *et al.* (Deutsche Physikalische Gesellschaft, Hamburg, 1965), Vol. II, p. 97. G. Bellettini, G. Cocconi, A. N. Diddens, E. Lillethum, J. P. Scanlon, A. M. Shapiro, and A. M. Wetherell, Phys. Letters 18, 167 (1965).
[17] S. L. Adelman, Phys. Rev. Letters 13, 555 (1964).
[18] S. L. Adelman, Phys. Rev. Letters 14, 1043 (1965).
[19] L. D. Roper, Phys. Rev. Letters 12, 340 (1964).
[20] P. Auvil, C. Lovelace, A. Donnachie, and T. A. Lea, Phys. Letters 12, 76 (1964).
[21] P. Bareyre, C. Bricman, A. V. Stirling, and G. Villet, Phys. Letters 18, 342 (1965).
[22] L. D. Roper, R. M. Wright, and B. T. Feld, Phys. Rev. 138, B190 (1965).
[23] B. H. Bransden, P. J. O'Donnel, and R. G. Moorhouse, Phys. Letters 11, 339 (1964).
[24] J. Cence, Phys. Letters 20, 306 (1966).
[25] R. H. Dalitz and R. G. Moorhouse, Phys. Letters 14, 159 (1965).

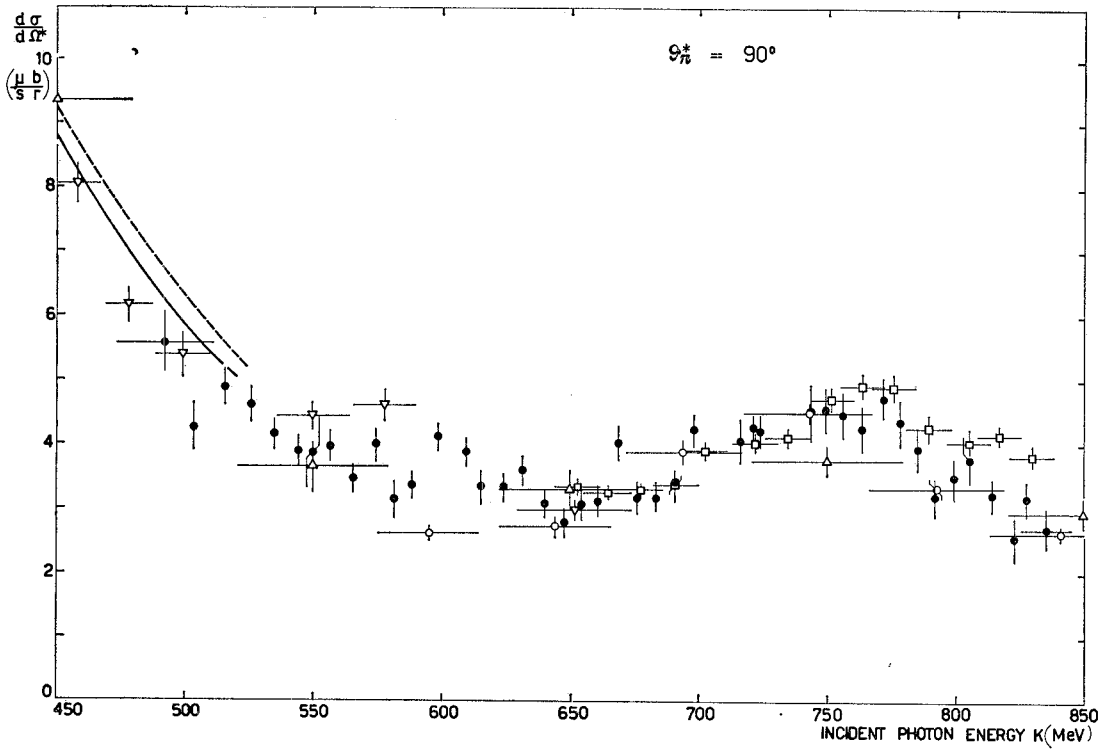

FIG. 13. Differential cross section results at $\theta_\pi^*=90°$. The different sets of measurements of Fig. 10 have been averaged (see Ref. 8). Results of previous p-π^0 coincidence experiments are also reported (see Ref. 11). The dashed and full lines are theoretical calculations by Schmidt (Ref. 12) and Donnachie and Shaw (Ref. 13), respectively. ● Present results; △ Ref. 10; □ Ref. 27; ○ Ref. 9; ▽ Y. Nagashima [thesis, University of Tokyo, Report No. INST-81, Th-47, 1964 (unpublished)]. The energy resolution of present results is shown on the first and last point.

The fact that we do not observe any bump below $E^*=1450$ MeV cannot be considered evidence against the presence of a P_{11} resonance in our channel: A very broad bump could in fact be masked between the tails of the first and second resonance.

In addition, one should remember that in photoproduction both an isoscalar and an isovector part contribute to each multipole. It may happen that those two contributions are of the same order but opposite in sign for the P_{11} resonance, so that the two contributions cancel each other.

If this is the case, the P_{11} resonance should be important in the photoproduction of pions on neutrons. The relative sign of the isoscalar and isovector contributions is in fact opposite when the photoproduction occurs on neutrons instead of on protons.[26]

We now look beyond $k=650$ MeV. We have collected data above 700 MeV only at 90°. In fact, at $\theta_\pi^*=120°$ and 135° the nuclear absorption of protons does not allow for the extension of the measurements up to this energy interval using a range telescope. In Fig. 15 (and Table IV) we show, together with our results, the results of the two other experiments[27,28] performed with a good energy resolution. All of them show a fast rise of the cross section at ~700 MeV followed by a flat region, and another rise around 740 MeV. This anomaly is not significant enough in each experiment considered separately, but may become significant as the results are considered together. Of course, if the anomaly exists, it could even be the manifestation of the P_{11} resonance in photoproduction; however, its width seems to be too small and its position too high for this explanation to be consistent with what is observed in other reaction channels.[15-17]

Considering that 710 MeV is just the threshold for η photoproduction, we tried to interpret the observed anomaly also in terms of a different mechanism, i.e., as a cusp effect due to the sharp opening of the η-photoproduction channel; this mechanism was first predicted by Rekalo[29] for π^0 photoproduction. In the following we will discuss this point of view.

[26] We thank Professor W. Schmidt for emphasizing this point to us.

[27] M. Deutsch, C. Mencuccini, R. Querzoli, G. Salvini, V. Silvestrini, and R. Stiening, in Proceedings of the Frascati Congress, 1962 (unpublished), p. 28.

[28] H. De Staebler, Jr., E. F. Erickson, A. C. Hern, and C. Schaerf, Phys. Rev. **140**, 342 (1965).

[29] M. P. Rekalo, Zh. Eksperim. i Teor. Fiz. **46**, 218 (1964) [English transl.: Soviet Phys.—JETP **19**, 152 (1964)].

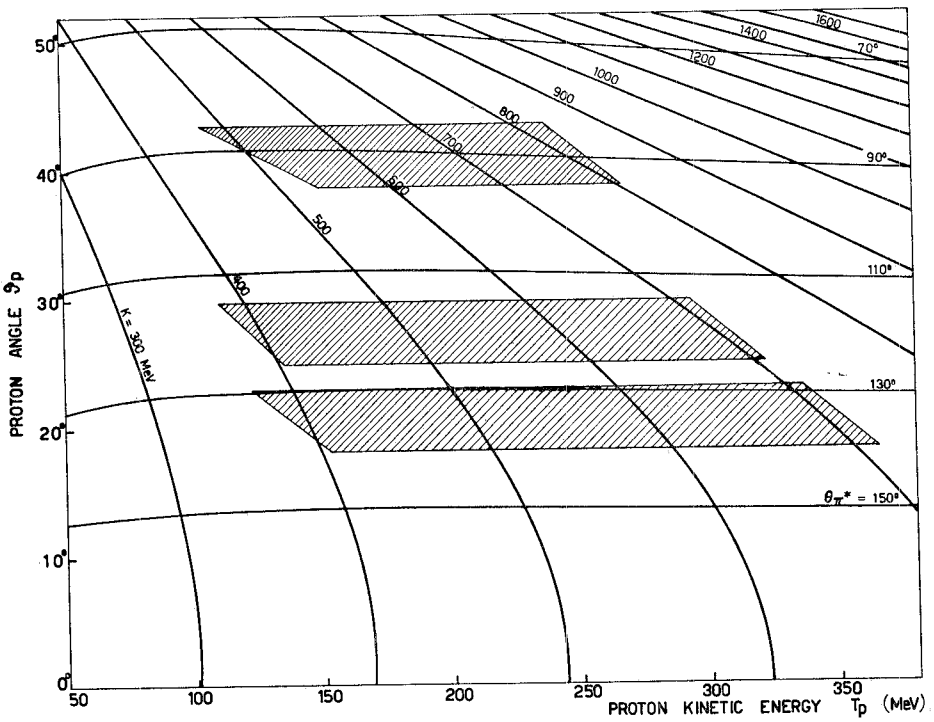

FIG. 14. Kinematical regions covered by the measurements performed in the present experiment.

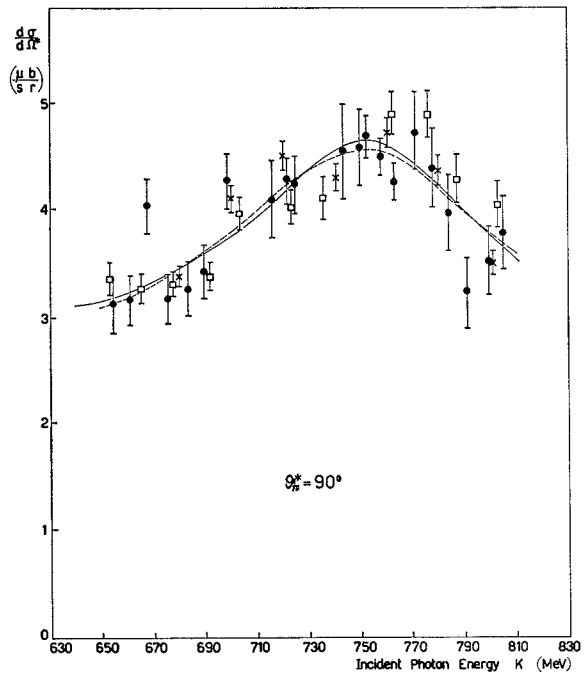

FIG. 15. The differential cross section for π^0 photoproduction at $\theta_\pi^*=90°$, in the energy interval 650–810 MeV, as obtained in three experiments performed with good energy resolution. The curves are best fits of the 90° differential cross section for π^0 photoproduction, assuming for the η-nucleon system an S_{11} resonant state at the η threshold. The resonant part of the second resonance multipoles M_{2-}, E_{2-} has been taken to be of the Breit-Wigner type (see Appendix B). ● Present results; □ Ref. 27; × Ref. 28; dashed line: $M_{2-}/E_{2-}=0$; full line: $M_{2-}/E_{2-}=\frac{1}{3}$.

The following facts[1] should be kept in mind:

(a) The π^0 photoproduction seems to occur, in this energy region, mainly in a $T=\frac{1}{2}$ isospin state, as does the photoproduction of η's.

(b) The η photoproduction cross section has a very fast rise near threshold.[30]

An exact calculation of the η cusp effect is not possible because of the present lack of knowledge of the multipoles which are important in photoproduction in the region of the second resonance. We have, however, tried a calculation using a simplified model (some details are given in Appendix B), which relies on a few basic assumptions which we outline as follows:

(1) As in Ref. 31 we assume that the η is produced near threshold in an S_{11} state. The η cusp effect should then reflect, in π^0 photoproduction, on the E_{0+} dipole.

(2) We neglect the multipion production, which seems to be justified by the behavior of the inelasticity parameter in the S_{11}.[20,21] We apply the unitarity and time-reversal invariance of the S matrix, disregarding all reactions except

$$\pi N \rightarrow \pi N;\quad \pi N \rightarrow \eta N;\quad \gamma N \rightarrow \pi N;\quad \gamma N \rightarrow \eta N;\quad \eta N \rightarrow \eta N. \tag{4}$$

[30] R. Prepost, Lundquist, and D. Quinn, in *Proceedings of the International Symposium on Electron and Photon Interactions at High Energies*, edited by G. Höhler *et al.* (Deutsche Physikalische Gesellschaft, Hamburg, 1965), Vol. II, p. 152.

[31] A. W. Hendry and R. G. Moorhouse, Phys. Letters 18, 171 (1965).

A set of equations is obtained, which have an unique solution[32] if we further assume that the η-N system is produced through a resonating state, in both input channels $\pi+p$ and $\gamma+p$; again according to Ref. 31, we have assumed that the S_{11} η-N resonance occurs at $E^*=1520$ MeV. In this way, the E_{0+} ($T=\frac{1}{2}$) multipole[33] can be determined in terms of measured quantities, i.e., the S_{11} π-N scattering amplitude and the η-photoproduction cross section. Information on the other multipoles necessary to build up the over-all π^0 photoproduction cross section has been extracted mainly from Refs. 12 and 13. The explicit expression of the cross section is given in Appendix B. In Fig. 15 the best fits we could obtain in the two cases $M_{2-}/E_{2-}=0$ (Ref. 34) or $\frac{1}{3}$ (Ref. 35) are compared with the experimental results. As we see, the computed curves do not fit the anomaly observed at $k\simeq 700$–740 MeV: The perturbation due to the η channel remains small, notwithstanding the sharp rise of the η-photoproduction cross section.

Apart from the doubts one could have that the observed anomaly is a fluctuation, the reason of the discrepancy could be found in the initial assumption of an S_{11} η-N resonant state, as well as in our approximations in calculating the anomaly. It is worthwhile to remember that the η-N system could even be in a different state, other than the S_{11}, and therefore the over-all situation could be more complicated. In particular a P_{11} resonant state, with even large interferences with other states, cannot be excluded. Some further remarks on this point are given in Appendix B.

In addition, as recently pointed out by several authors,[36–38] the D_{13} state could also be important in the η photoproduction, in which case a naive approach could be even more inadequate.

6. CONCLUSIONS

We summarize our results and discussion in the following points:

(1) Measurements of the π^0 photoproduction cross section have been performed by us with good energy resolution.

(2) The π^0 photoproduction cross section seems to be well described by the theoretical calculations based on dispersion relations[12,13] up to $k=550$ MeV of the incident photon ($E^*=1380$ MeV total energy in the center-of-mass system).

(3) We do not see any significant evidence of a new isobaric state like the P_{11} state observed in many experiments[15–17] and as indicated by the results of phase-shift analysis,[18–23] at c.m. total energies smaller than 1480 MeV.

(4) There is an experimental indication (see Fig. 15) of a possible structure in the region of the second resonance at $k=700$–740 MeV. We tried to interpret it as an η cusp effect. A rough estimate, assuming that the η is produced near threshold in an S_{11} resonant state, predicts an anomaly much smaller than the observed one. A possible reason for this discrepancy could be that the η-N system is at the threshold in a different state, other than S_{11} state. In particular, a P_{11} resonant state with interferences with other states cannot be excluded according to the experimental information available up to now.

ACKNOWLEDGMENTS

Thanks are due to Professor W. Schmidt for valuable critical remarks and suggestions. We wish to thank, V. Bidoli, I. Bruno, and M. Massimi, our technicians, for their assistance in setting up the apparatus and maintaining it during its long operation. The skill and patience of Mr. and Mrs. F. Melorio, and E. Paganelli, the scanners, are also acknowledged. Finally, we wish to thank the synchrotron staff for their collaboration during our runs.

APPENDIX A

In addition to the statistical errors quoted in Figs. 11–13 and in Tables I–III, other kinds of errors do affect our results.

However, since all these errors, except the statistical ones, are constant or have a smooth behavior as a function of energy, our discussion in Sec. 5, in which the absolute normalization was not of relevant importance, was based on the results affected by the statistical errors only.

The most important sources of errors we could think of, in addition to statistics, are the following.

(1) *Calibration of the Wilson quantameter.* We believe our quantameter to be accurate to $\pm 5\%$. An error in its calibration would affect our results by a constant factor, independent of energy.

(2) *π^0's not detected by C due to the electronics threshold.* By extrapolating below threshold the pulse-height distributions in C (Fig. 6), we have evaluated this correction as being, for $\theta_\pi^*=135°$, 10% at $k=400$ MeV, going smoothly to 4% at $k\simeq 700$ MeV; for $\theta_\pi^*=120°$, 10% at $k=400$ MeV, going smoothly to 4% at $k\simeq 700$ MeV; and for $\theta_\pi^*=90°$, 5% at $k=550$ MeV, going smoothly to zero at $k\simeq 850$ MeV. Our evaluation of the error in this correction is $\pm 60\%$ of the correction itself.

(3) *Nuclear interactions.* We have used a mean free path for nuclear interactions of protons in aluminum, $\lambda=110$ g/cm^2. This value of λ is affected by an error, since it is extracted from the results of an experiment[5] performed in a different geometrical situation than ours. We have analyzed data using for λ the values of 80 g/cm^2 and 140 g/cm^2: This is, in our opinion, the

[32] C. Mencuccini and A. Reale, Nuovo Cimento 48, 579 (1967).
[33] Here and in the following we use for the multipoles standard notations ($E_{l\pm}$; $M_{l\pm}$ are defined, for instance, in G. F. Chew, M. L. Goldberger, F. E. Low, and Y. Nambu, Phys. Rev. **106**, 1345 (1957)).
[34] Ph. Salin, Nuovo Cimento **28**, 1294 (1963).
[35] D. S. Beder, Nuovo Cimento **33**, 94 (1964).
[36] W. B. Richards, C. B. Chiu, R. D. Eandi, A. C. Helmholz, R. W. Kenney, B. J. Moyer, J. Poirier, R. J. Cence, V. Z. Peterson, N. R. Sehgal, and V. J. Stenger, Phys. Rev. Letters **16**, 1221 (1966).
[37] S. Minami, Phys. Rev. **147**, 1123 (1966).
[38] G. Altarelli, F. Buccella, and R. Gatto, Nuovo Cimento **35**, 331 (1965).

TABLE V. Effect of a possible error in λ on our results. For instance, at 135°, increasing λ by 27% (from λ=110 to λ=140 g/cm²) would decrease the cross section by an amount which goes smoothly from 1.0% at $k=400$ MeV, to 4.5% at $k=500$ MeV, etc.

θ_π^*	$\delta\lambda$	$\Delta\sigma/\sigma$	$\Delta\sigma/\sigma$	$\Delta\sigma/\sigma$	$\Delta\sigma/\sigma$
		at $k=400$	at $k=500$	at $k=600$	at $k=700$
135°	+27%	−1.8%	−4.5%	−5.5%	−12.5%
	−27%	+3.8%	+8.2%	+10.0%	+27.9%
120°	+27%	−1.8%	−3.3%	−4.2%	−10.4%
	−27%	+2.0%	+5.9%	+7.1%	+21.1%
		at $k=525$	at $k=680$	at $k=820$	
90°	+27%	+1.5%	−2.0%	−8.4%	
	−27%	−3.1%	+3.0%	+16.6%	

maximum range of values for λ in our conditions. The results are summarized in Table V. As one can see, using a value of λ of 95–100 g/cm² would bring our points at higher energy ($\theta_\pi^*=120°$) into agreement with previous results, leaving unaffected the agreement of the other points (at the three angles).

APPENDIX B

We report here some details on the calculation performed to estimate the η cusp effect. A full account can be found in Ref. 32.

Assuming that only the multipoles E_{0+}, M_{1+}, E_{2-}, and M_{2-} are important in the region of the second resonance, the 90° differential cross section for reaction (1) can be written

$$\frac{K}{q}\left(\frac{d\sigma}{d\Omega^*}\right)=|E_{0+}|^2+\tfrac{5}{2}|M_{1+}|^2+\tfrac{5}{2}|E_{2-}|^2+\tfrac{9}{2}|M_{2-}|^2 -\mathrm{Re}[E_{0+}{}^*(E_{2-}-3M_{2-})]+3\,\mathrm{Re}[M_{2-}{}^*E_{2-}], \quad \text{(A1)}$$

where K and q are the c.m. momenta of the photon and meson, respectively.

The E_{0+} multipole has been evaluated under the assumptions listed in Sec. 5. Let us write it in the form

$$E_{0+}=\tfrac{2}{3}E_{0+}{}^{3/2}+\tfrac{1}{3}Ce^{i\gamma_0}.$$

The $E_{0+}{}^{3/2}$ part, which is not expected to change very fast in our energy region, has been extrapolated from Refs. 12 and 13; C and γ_0 were determined from the known amplitudes of the reactions (4), using the unitarity and time-reversal invariance of the S-matrix. The first resonance multipole M_{+1} has been taken from Refs. 12 and 13.

Concerning the ratio $r=M_{2-}/E_{2-}$ of the magnetic to the electric $T=\frac{1}{2}$ amplitude, we considered both the cases $r\simeq 0$ [case (a)] and $r\simeq\frac{1}{3}$ [case (b)]. The first case is suggested by Ref. 34; the second one is even more firmly supported by theoretical analyses[35,39] which need a $\frac{1}{3}$ ratio to explain the experimental results of the forward π^0 photoproduction cross section.[40] The $T=\frac{3}{2}$ nonresonating part of the E_{2-} multipole has been taken from Refs. 12 and 13. For the resonating $T=\frac{1}{2}$ part of this multipole we assumed a Breit-Wigner (BW) shape:

$$\frac{B\Gamma E_{\rm res}}{(E^2-E_{\rm res}{}^2)+i\Gamma E_{\rm res}}.$$

The amplitude B and the width Γ are free parameters to be determined by best fitting with (A1) the experimental results in the energy region 650÷800 MeV (Fig. 15 and Table IV). The resonance energy was $E_{\rm res}=1518$ MeV, as suggested in Ref. 21.

However, this fit is in rather bad agreement with our data. To improve the fit, we tried to take into account background amplitudes from the previously neglected multipoles and their interference with the BW or E_{0+} terms. Only the real parts of the amplitudes have been considered.

Therefore, the additional quantity

$$\alpha\,\mathrm{Re}(BW)+\beta\,\mathrm{Re}E_{0+}+\gamma$$

was added to (A1); α, β, and γ are real energy-independent coefficients, which stand for rather cumbersome combinations of those smaller multipoles.

The best fits obtained by varying B, Γ, α, β, and γ are shown in Fig. 15. The resulting sets of important parameters are: case (a)—($r=0$), $\chi^2=72$ (33 degrees of freedom), $\Gamma=80$ MeV; $B/(10^{-2}\lambda_\pi)=0.8$; case (b)—($r=\frac{1}{3}$), $\chi^2=73$ (33 degrees of freedom), $\Gamma=80$ MeV; $B/10^{-2}\lambda_\pi)=0.5$, $\lambda_\pi=$Compton wave length of the π. We did not try to get a better fit because this result would be achieved by increasing the number of independent parameters, but then the whole procedure would lose information. In conclusion, the variation of the E_{0+} multipole as a function of the energy, going through the η threshold, is not great enough to explain the observed anomaly. Unless a more refined treatment shows that this anomaly arises from a complicated interference of all the multipoles which are present, one is forced to calculate the cusp effect on using different assumption.

For instance, one could assume a P_{11} bound state for the η-N system. This possibility cannot be excluded by the present experimental evidence. In fact, the assignment of the orbital angular momentum to the η-N system was mainly based on the fact that the S_{11} wave, in π-N scattering, shows an inelasticity parameter changing abruptly from 1 just at the opening of the η production channel. However, mainly according to Ref. 24, also the P_{11} inelasticity parameter changes enough to allow the opening of the η-production channel. Further information can be obtained by an analysis of the η-production cross section as a function of the energy just near threshold.

On these lines, some authors[41] are in favor of an S_{11} state; however, we tried a similar analysis, and found that the hypotheses of both an S_{11}-state η-N real resonance and of a P_{11}-wave bound state below threshold are consistent.

[39] A. Bietti, Phys. Rev. **142**, 1258 (1966).

[40] F. Talman, C. Clinesmith, R. Gomez, and A. Tollestrup, Phys. Rev. Letters **9**, 177 (1963).

[41] F. Uchiyama-Campbell and R. K. Logan, Phys. Rev. **149**, 1220 (1966).